Initial Mediterranean response to major climate reorganization during the last interglacial-glacial transition

Celia Martin-Puertas[1*,2], Stefan Lauterbach[3], Judy R.M. Allen[4], Marta Perez[1], Simon Blockley[1], Sabine Wulf[5], Brian Huntley[4] and Achim Brauer[2, 6]

[1] Department of Geography, Royal Holloway University of London, Egham, Surrey TW20 0EX, UK.

[2] Section Climate Dynamics and Landscape Evolution, GFZ German Centre for Geosciences, 14473 Potsdam, Germany

[3] Leibniz Laboratory for Radiometric Dating and Stable Isotope Research, Kiel University, 24118 Kiel, Germany

[4] Department of Biosciences, University of Durham, Durham DH1 3LE, UK

[5] Department of Geography, University of Portsmouth, Portsmouth PO1 3HE, UK

[6] Institute of Geosciences, University of Potsdam, 14476, Germany

*corresponding author: celia.martinpuertas@rhul.ac.uk

Abstract

Millennial-scale Dansgaard Oeschger (DO) variability at northern high latitudes has influenced climatic and environmental conditions in the Mediterranean during the last glacial period. There is evidence that the hemispheric transmission of the DO variability occurred at the end of DO event 25; however, the exact timing and the trigger that activated the environmental response in the Mediterranean remains incompletely understood. Here, we provide evidence that the clear millennial-scale teleconnection between Greenland and the Mediterranean started at ~111.4 ka BP and was initiated by a sub-millennial scale cooling in Greenland (GI-25b). High-resolution sediment proxies and the pollen record of Lago Grande di Monticchio (MON), Italy, reflect climatic instability during the last millennium of the last interglacial, which was characterised by a first and short cooling episode (MON 1) at 111.44 ± 0.69 ka BP, coinciding with the Greenland cold sub-event GI-25b in duration and timing (within dating uncertainties). MON and Greenland (NorthGRIP ice core) also agree in recording a subsequent warm rebound phase that abruptly culminated in the stadial MON 2 / GS-25, marking the transition into the last glacial period. Our results show that the GI-25b triggered an early environmental response at MON to centennial-scale climate change in Greenland as a prelude to the millennial-scale teleconnection that was maintained during the glacial period.

Keywords: Palaeoclimatology, Last Interglacial-Glacial transition, millennial-scale variability, Mediterranean, varved sediments

1 Introduction

The transition from the Last Interglacial (LI) into the Last Glacial in the Northern Hemisphere (NH) developed differently from polar to subtropical regions. While the initial build-up of the NH ice sheets started ~122 thousand years before AD 2000 (ka b2k) (NGRIP MEMBERS, 2004; Rasmussen et al., 2014) and was associated with declining northern summer insolation, southern European climate remained warm and relatively stable until ~110 ka AD 1950 (BP) when a dramatic shift in the environment marked the end of the LI in this region (Woillard, 1979; Kukla et al., 1997; Shackleton et al., 2002; Shackleton et al., 2003; Tzedakis, 2003; Sánchez-Goñi et al., 2005; Brauer et al., 2007). This change corresponds to a biostratigraphic boundary that defines the transition to what is known as the Mélisey I stadial in central and southwestern European pollen records (Woillard, 1979; Kukla et al., 1997). The direct correlation between the European biostratigraphy and marine proxy-based stratigraphies (i.e. North Atlantic ice-rafted detritus (IRD), stable isotopes and sea surface temperature) developed by Sánchez-Goñi et al. (2005), Shackleton et al. (2002) and Shackleton et al. (2003) revealed that (1) the North Atlantic cold event C26 at ~119 ka BP was associated with a western European cooling marked by the increase of hornbeam trees within an oak-dominated forest at 42°N and probably the spread of cold-tolerant trees in Europe north of 50°N and (2) the Mélisey I stadial and the North Atlantic cold event C24 at ~110 ka BP occurred contemporaneously. Recently, Martin-Puertas et al. (2014) correlated the Mélisey I with Greenland stadial GS-25 (Greenland event stratigraphy, NGRIP members, 2004; Rasmussen et al., 2014). GS-25 (Greenland ice-core event stratigraphy), C24 (North Atlantic sea surface temperature stratigraphy) and Mélisey I (central Europe pollen stratigraphy) are the regional representatives of the first abrupt climatic oscillation within a series of millennial-scale climatic fluctuations in the NH during the last glacial period, known as Dansgaard Oeschger (DO) events (McManus et al 1994; Chapman and Shackleton, 1999; NGRIP MEMBERS, 2004, Oppo et al., 2006; Capron et al., 2012). DO events typically consist of an abrupt warming

78 followed by an interval of mild conditions (Greenland interstadial, GI) and a gradual cooling
79 that culminates in a cold phase (Greenland stadial, GS). The duration of the GI and GS varies
80 between a century and a few millennia (Sánchez Goñi and Harrison, 2010; Wolff et al., 2010;
81 Rasmussen et al., 2014). This millennial-scale variability is linked to changes in the strength of
82 the Atlantic Meridional Overturning Circulation, which influences the climate globally
83 (Broecker, 1998, Barker et al., 2011). Prior to GS-25, a weak cold phase (GS-26) occurred
84 between 119.14 and 115.37 ka b2k (NGRIP MEMBERS, 2004; Rasmussen et al., 2014) with
85 presumed counterparts in the subtropical Atlantic Ocean (cold event C26) (Chapman and
86 Shackleton, 1999) and in northern, western and central Europe (Chedaddi et al., 1998;
87 Sánchez-Goñi et al., 2005). At centennial time scales, the updated INTIMATE event
88 stratigraphy from the Greenland ice cores proposes a further sub-division of the following
89 warm interval GI-25 into three sub-events: GI-25c (115.37–111.44 ka b2k); GI-25b (111.44–
90 110.94 ka b2k); and GI-25a (110.94–110.64 ka b2k) (Rasmussen et al., 2014). GI-25c
91 represents the main warm phase of DO 25, while GI-25b reflects a 500-year cooling episode,
92 which was followed by GI-25a, a 300-year rebound preceding the stadial phase GS-25 that
93 corresponds to the cooling stage of DO 25.
94 Palaeotemperature records from the North Atlantic Ocean reflect a weak and short cooling
95 episode (cold event C25) associated with a weak IRD event prior to cold event C24
96 (McManus et al., 1994; Chapman and Shackleton 1999). Assuming a correlation between
97 cold event C24 and Mélisey I, Lehman et al. (2002) correlated the cold event C25 to an
98 abrupt transition from deciduous trees to taiga forest in the pollen record of Grande Pile
99 (France), known as the Woillard event (WE) (Woillard, 1979), suggesting that the WE was as
100 a consequence of changes in the Atlantic temperature altering climate and vegetation in
101 Europe. The WE is dated at ca. 111 ka BP in Grande Pile (Kukla et al., 1997) and lasted about
102 300 ± 150 years (Woillard, 1979; Kukla et al., 1997). In the Mediterranean, the pollen record
103 of Lago Grade di Monticchio (MON) shows millennial- to centennial-scale variations, which

were correlated with the Grande Pile pollen record, adopting the same nomenclature (Brauer et al., 2007). The WE was identified in the MON pollen record centred at 111.16 ± 5.55 ka BP with an estimated duration of ca. 320 years (Brauer et al., 2007; Allen and Huntley, 2009), but it is represented by a single pollen sample only. Therefore, the duration estimate of the WE in the MON pollen record is limited by pollen data resolution, as we will discuss below. Most recently, a Mediterranean speleothem (BMS1) from Bue Marino Cave, Sardinia, Italy, provided evidence for a cool episode centred at 112 $^{+0.52}/_{-0.59}$ ka followed by warmer conditions at 111.76 $^{+0.43}/_{-0.45}$ ka, which were correlated with the Greenland sub-events GI-25b and GI-25a, respectively (Columbu et al., 2017). Both, the MON and BMS1 proxy records are independently dated, which allows reliable estimates of the duration of the climatic oscillations and comparison with the Greenland ice cores without *a priori* assuming synchronicity of the events. While the BMS1 stable isotope record reveals hydroclimatic and temperature information, the MON sediment sequence reflects climate-induced environmental changes and the preservation of varves in the lacustrine sediments allows us to develop a multi-proxy approach even at seasonal resolution (Brauer et al., 2007; Martin-Puertas et al., 2014).

Here we present an updated and detailed study of the final phase of the LI from the MON varved sediments. We have extended the high-resolution proxy records published by Martin-Puertas et al. (2014) from ca. 111.4 ka BP back to ca. 120 ka BP and evaluate sub-millennial-scale climate variability during the last glacial inception. Our objectives are to: (1) double check the occurrence of the WE in the MON proxy records; (2) evaluate differences in proxy response (pollen vs. sediment proxies) to sub-millennial-scale climate variability in order to define the change points more precisely; and (3) estimate the onset of the teleconnection between the initial build-up of the NH ice sheet and its environmental impact on the Mediterranean beyond the well-established correlation at millennial time scales. For this

129 particular objective, we have avoided wiggle matching of the climatic oscillations and have
130 compared high-resolution proxy records that are independently dated.
131 [Fig. 1]
132
133 **2 Site description and Methods**
134 *2.1 Study site*
135 Lago Grande di Monticchio (40°56' N, 15°35' E, 656 m a.s.l.) is a maar lake formed during the
136 final phreatomagmatic eruptions of Monte Vulture volcano (southern Italy) about 132,000
137 years ago (Brocchini et al., 1994; Stoppa and Principe, 1998). Maximum water depth is 36 m,
138 but much of the lake is a shallow shelf sloping from the shoreline towards 12 m depth from
139 where the cores were taken (Allen et al., 1999; Brauer et al., 2007). The lake area is 0.4 km^2;
140 its catchment, which is mainly composed of K-alkaline phonotephrites, covers 2.37 km^2. The
141 maximum elevation in the catchment is 956 m a.s.l., with a maximum relief of 300 m. The lake
142 is spring fed and thus regulated by the local groundwater system and by rainfall and surface
143 runoff. Mediterranean summer drought might cause the lake level to lower (Hutchinson,
144 1970).
145 *2.2 Sedimentological analyses*
146 The MON sediment record is ~130 m long. We have worked on a sequence of 5 m length
147 between 79 and 84 m sediment depth of the composite profile J/M/O, which combines the
148 best-preserved sequences of sediment cores J, M and O (Fig. 1b) (Martin-Puertas et al., 2014).
149 Varve counting and microfacies analyses were done on sediment thin sections using a
150 petrographic microscope (Brauer et al., 2007; Martin-Puertas et al., 2014). The geochemical
151 composition of the sediments was obtained by micro X-ray fluorescence (XRF) scanning of the
152 10-cm long impregnated sediment blocks that were used to produce the thin sections
153 mentioned above, allowing direct comparison of element abundances with microfacies data.

154 The analytical system used for elemental scanning was an EAGLE III XL μ-XRF spectrometer
155 deployed at the GFZ Potsdam (see details in Brauer et al., 2007).

156 *2.3 Pollen analyses*

157 Thirteen new pollen samples taken between 80.45 and 80.70 m sediment depth have been
158 analysed following standard methods applied in previous pollen studies at the site (Allen et
159 al., 1999; Brauer et al., 2007; Allen and Huntley, 2009) in order to increase the temporal
160 resolution of the pollen record published by Brauer et al. (2007) between 111.25 and 111 ka
161 BP, where the WE was assuned by Brauer et al. (2007). We integrated the new pollen samples
162 into the previous pollen record in order to get a sample resolution higher than 20 years
163 (according to the age-depth model). In the particular case of peak previously correlated to the
164 WE, we have increased the sample resolution to 5 years (average sedimentation rate is 0.39
165 mm / year) by adding four contiguous samples below and four additional samples above the
166 published sample that reflects the WE. We have also calculated pollen influx defined as the
167 number of pollen grains accumulated per unit of sediment surface area and per unit of time
168 (grains x cm^{-2} x $year^{-1}$) in order to get a semi-quantitative measure of both vegetation
169 distribution and abundance (Davis et al., 1972; Hicks and Hyvärinen, 1999). Anomalies in the
170 proxy records were considered significant where increases or decreases are greater than
171 twice the standard deviation of the proxy dataset.

172 *2.4 Chronology*

173 The most recent version of the MON varve chronology for the interval comprising the
174 transition from the LI into the LG (MON-2014; ca. 76 to 111.4 ka BP; 50.22–81.53 m sediment
175 depth) was published by Martin-Puertas et al. (2014). Varves were counted on the composite
176 profile J/M/O using an accurate counting method based on detailed sediment microfacies
177 analysis (100x microscopic magnification) and the measurement of the thickness of the
178 different sub-layers constituting the varves. In this study we extended the MON-2014
179 chronology down to 84 m sediment depth using the same counting method. In order to

provide a relative counting error as uncertainty range for the duration of the climatic phases that are discussed below, we compared the different varve counts available for the MON sediment record during the study interval between 79.00 and 84.00 m sediment depth. Those are MON-07 (79.00–84.00 m; Brauer et al., 2007), MON-2014 (79.00–81.53 m; Martin-Puertas et al., 2014) and the new count (81.53–84.00 m; this study). In terms of absolute age uncertainty, the MON varve chronology was validated by tephrochronology and its absolute uncertainty is up to 5% according to the 2σ error calculated by the discrepancy between the mean radiometric / radioisotopic and varve ages of tephra layers identified in the MON sediments (Wulf et al., 2012). As a new contribution to the MON chronology, we have applied Bayesian age-depth modelling for a more thorough integration of the varve and tephra records, aiming at minimising the absolute age uncertainty during the study interval (109–120 ka BP) as much as possible (<5%). For this purpose, we ran a P_Sequence deposition model implemented in OxCal 4.2 (Bronk Ramsey, 2008) and included recently updated $^{40}Ar/^{39}Ar$ dates for the Mediterranean marine tephra correlatives X-5 (106 ± 1.3 ka BP, Giaccio et al., 2012) and X-6 (109.5 ± 0.9 ka BP, Regattieri et al., 2017) for the dated points in the model and the last relative varve time scale as the Z value in the model (Bronk Ramsey, 2008; Blockley et al., 2008). As the model is based on relative varve numbers we have not included interpolation modelling (Table 1, Fig. 2).

3 Results, age modelling and discussion of the presumed Woillard Event in the Lago Grande di Monticchio sediment record

A total of 8500 varves were counted from 81.53 to 84.00 m sediment depth, which extends the previously published MON-2014 chronology back to ca. 120 ka BP. The maximum cumulative counting error (i.e. the differences between the three varve time scales where they overlap) at the base of the study interval was ± 386 varves. As this counting error is lower than the modelled uncertainty at tephra layer X-6 (± 697 years) (Table 1), we have considered

206 the latter as the maximum absolute age uncertainty for the entire study interval, and the age
207 given by the varve time scale as the most reliable date for the observed oscillations. Thereby,
208 it has been possible to reduce the absolute age uncertainty from 5% down to 1.2%.
209
210 [Fig. 2]
211
212 Figure 3 shows a set of sedimentological, geochemical and pollen data from the MON
213 sediment sequence as indicators of environmental and climatic processes affecting the
214 lacustrine system, and changes in the surrounding landscape, from 120 to 109 ± 0.69 ka BP.
215 The rapid reduction in woody taxa pollen (60–40 %) at 110.43 ± 0.69 ka BP represents the
216 onset of the Mélisey I stadial and the biostratigraphic end of the LI in the MON sediment
217 record (Brauer et al., 2007; Allen and Huntley, 2009). The WE at MON was associated with a
218 rapid but transient decrease in woody taxa pollen (from 95% to 70%), with grassland
219 expanding on some part of the catchment, that occurred towards the end of pollen sub-zone
220 LPAZ 21a and ca. 700 years before the onset of Mélisey I / LPAZ 20 (the MON pollen
221 stratigraphy is fully described in Allen and Huntley [2009]).
222
223 [Fig. 3]
224
225 Although the reduction in woody taxa pollen is less pronounced than during Mélisey I, the WE
226 fluctuation in the pollen record was interpreted as a cool and dry episode within a warm
227 period (Allen and Huntley, 2009). In line with our first objective, new pollen samples were
228 added to verify the signal of that fluctuation, which is so far based on one single pollen sample
229 only (Fig. 4). The analyses of the new pollen samples confirm the existence of a change in
230 pollen data which is represented by four contiguous pollen samples that indicate a minor
231 reduction in the amount of tree pollen taxa from 111.185 to 111.150 ± 0.69 ka BP. This is

supported by a negative oscillation in woody taxa pollen influx and woody taxa percentages (Fig. 4a). Both the transitions at the beginning and end of this fluctuation occurred in less than 8 and 13 varve years, respectively (Fig. 4a). This fluctuation was, however, much shorter than previously assumed, *i.e.* 40 ± 5 years instead of the ca. 320-year oscillation reported by Allen and Huntley (2009). Considering this new information, we suggest that this fluctuation was too short to encompass a transition from forest to grassland and a subsequent return to forest. I is more likely that the pollen data reflect a short episode of reduced tree pollen production. Such an episode may reflect a short-lived shift in climatic conditions, sufficient to reduce the vigour of the trees and hence also reduce their flowering, but not sufficient to cause their death before climate conditions reverted once again to favour the trees.

Another reason to revise the correlation of this episode with the WE defined in Grande Pile (France) is based on chronology. The WE in Grande Pile preceded the transition to Mélisey I by four millennia (Kukla et al., 1997), while the observed tree pollen decline at Monticchio occurs only ca. 700 years before Mélisey I was only ca. 700 years (Brauer et al., 2007; Allen and Huntley, 2009). As both chronologies are based on annual layer counts, these two events in the pollen records are therefore unlikely to reflect the same climatic signal.

[Fig. 4]

Martin-Puertas et al. (2014) reported that the assumed WE in the MON pollen record coincided with the first cooling period at the end of the last interglacial identified in the sediment proxies, *i.e.* MON 1 (111.23–111.01 ± 0.69 ka BP; Martin-Puertas et al., 2014). These proxies indicate stadial-like (cold) conditions through the deposition of thick siderite varves (microfacies 2b in Martin-Puertas et al., 2014), while thin organic-diatomaceous varves (microfacies 1a in Martin-Puertas et al., 2014) occurred during interglacial (warm) and interstadial (mild) conditions. The downcore extended dataset presented in this study,

however, revealed a short preceding phase of thick siderite varves, which appeared already ca. 220 years earlier at 111.45 ka BP and lasted until 111.39 ± 0.69 ka BP (Fig. 3, 4b). Therefore, we must re-define MON 1 as a slightly longer cool period with a duration of 440 ± 9 years, lasting from 111.45 to 111.01 ± 0.69 ka BP compared to earlier reports defining MON 1 from 111.23 – 111.01 ± 0.69 ka BP (Martin-Puertas et al., 2014). The brief 40 ± 5 year decline in tree pollen that we constrained by our new high-resolution pollen analyses occurred in the middle of MON 1 and consequently we interpret this phase as an integral part of MON 1. The first truly stadial episode recorded in the sediments occurred about 1000 years later and is termed MON 2 (110.43 – 108.63 ± 0.69 ka BP). MON 2 agrees in timing and duration with Mélisey I in the MON pollen record (Fig. 3; Fig. 6 in Martin Puertas et al., 2014) and marks the end of the last interglacial as defined by biostratigraphy (Brauer et al., 2007). Both MON 1 and MON 2 are characterised by an increase in varve thickness and the occurrence of an annual authigenic siderite layer (represented by higher Fe/Ti ratios, Fig. 4). However, MON 1 and MON 2 are geochemically different. The Fe/Ti ratio and Ti counts are considerably higher during MON 2, indicating detrital input (Ti) as the main control of varve thickness variability (Martin-Puertas et al., 2014). Ti counts do not show a noticeable increase during MON 1 and Fe/Ti ratios mirror the changes in varve thickness (Fig. 3). Siderite precipitation in both MON 1 and MON 2 is interpreted as a response to colder and drier climate (i.e. stadial-like conditions). Lower evapotranspiration under stadial-like conditions might increase the water budget around the lake, favouring Fe input by groundwater. Additionally, cooler conditions might favour water column stratification, *i.e.* anoxic conditions at the lake bottom, by either relative lake level rise or reduction of lake water circulation due to winter ice cover. The combination of Fe input and hypolimnic anoxia under cooler conditions could have triggered siderite precipitation (Ohlendorf et al., 2000). A likely explanation for higher detrital input during MON 2 could be the opening of the forest cover that characterised the Mélisey I stadial and could have led to increased soil erosion. In contrast, MON 1 was apparently not associated with a persistent

large-scale reduction in tree pollen abundance, presumably because this cooling episode occurred during still prevailing interglacial conditions when the forest remained dense. This is well expressed by the lack of a Ti increase even during the short-lived fluctuation in pollen discussed above (Fig. 3), showing that soil erosion did not increase during that period. This evidence supports the idea that the pollen fluctuation most likely represents only a temporary decrease in woody taxa pollen production rather than a catchment-scale shift in vegetation structure. In addition, the fact that MON 1 occurred about 1000 years before MON 2 / Mélisey I, a stadial period that can be unequivocally linked to the Grand Pile pollen record, supports the conclusion that MON 1 reflects a different climatic oscillation than the WE, which occurred much earlier in Grand Pile (ca. 4000 years before Melisey 1). Examining the MON pollen record for the interval around 4000 years before the transition to Mélisey I reveals a minor single sample fluctuation dated to 113.70 kya BP (Allen & Huntley, 2009) that may correspond to the WE fluctuation at Grand Pile (Fig. 3). This possibility requires further investigation.

During the ca. 585-year interval between the end of MON 1 and the onset of MON 2, interglacial-type varves were again deposited, but these are slightly thicker than during full interglacial conditions (Fig. 3). We call this interval from 111.01 to 110.43 ± 0.69 ka BP 'MON-rebound 1' and assume that it reflects a moderate environmental improvement after the cool period that, however, did not reach full interglacial conditions.

Apparently, the climate-proxy relationship was not stationary during the study interval. The interpretation of the sedimentological proxies reveals shifting varve facies and varve thickness variability as a response to changes in temperature and lake circulation prior to the transition to Mélisey I. But after that time varve proxies were more sensitive to soil erosion and land surface processes. The pollen response to climatic conditions also seems to be different depending on the time scales of the forcing mechanisms. Whereas pollen variability generally reflects changes in vegetation composition and structure, most often in response to climatic changes at centennial to millennial time scales (e.g. interstadial-stadial variability), at annual

310 to decadal time scales, pollen may reflect variations in pollen production of different taxa
311 resulting from climatic variability (Huusko and Hicks, 2009). The fact that the observed short-
312 term decrease in pollen productivity at 111.18 ± 0.69 ka BP coincided with the most persistent
313 peak in siderite precipitation during that interval (Fig. 4) suggests that it was caused by cooler
314 climatic conditions. This further shows that, at MON, lake circulation was more sensitive to
315 low-amplitude climate change during the final stage of the LI than the composition of
316 catchment vegetation. For this reason, we defined the boundaries of decadal to centennial
317 climatic oscillations in the MON sediment record based on sediment proxies and not pollen.
318

319 **4 Regional and hemispheric comparison: palaeoclimatic implications**

320 The presence of the short-lived interval MON 1 at 111.44 ± 0.69 ka BP is the first signal of
321 environmental change at the very end of the LI in MON that we assume to be triggered by the
322 climatic deterioration. A detailed comparison of the MON record with the independently
323 dated high-resolution BMS1 speleothem from Bue Marino Cave in Sardinia (Columbu et al.,
324 2017), 550 km west of MON, provides further insights into the origin of the succession of a
325 cool (MON 1) and a mild (MON-rebound 1) interval (Fig. 5). The speleothem BMS1 is a three
326 millennia long record from ~113 – 110 ka with a growth hiatus at 111.76 $^{+0.43}$ / $_{-0.45}$ ka. The
327 BMS1 stable isotope data are interpreted as a proxy for precipitation and temperature with
328 higher $\delta^{18}O$ / higher $\delta^{13}C$ values indicating cool-dry conditions (Columbu et al., 2017). Both
329 records describe synchronous (within age uncertainties) sub-millennial-scale variability, which
330 strongly support the inference that the MON lake system was very sensitive to regional
331 climate change. Figure 5 also shows a recently published $\delta^{18}O$ isotope record of a speleothem
332 from Corchia Cave in Italy, 580 km northwest of MON, which is interpreted in terms of rainfall
333 amount (Drysdale et al., 2007; Tzedakis et al., 2018). The cold-dry (MON 1) oscillation and the
334 subsequent rebound, as well as the abrupt end of the LI (MON 2, yellow dashed line in Fig. 5)
335 are not recorded in the Corchia Cave speleothem. Instead, the Corchia Cave isotope data seem

to respond to a long-term gradual trend toward drier conditions at the end of the LI, suggesting that either this proxy-record might not be sensitive to sub-millennial-scale climate variability at that time or that climate change was regionally different.

[Fig. 5]

On a hemispheric scale from Northern to Southern Europe, Columbu et al. (2017) correlated the two rapid and short-lived climatic oscillations recorded in Bue Marino Cave with the Greenland sub-events GI-25b and GI-25a described by Rasmussen et al. (2014), based on the agreement between the independent dating of the isotopic records of Bue Marino Cave, the NGRIP ice core and the NALPS speleothem record (Boch et al., 2011). The onsets of GI-25b in Greenland and its counterparts in the Mediterranean date to 111.44 ± 2.78 ka b2k (111.39 ± 2.78 ka BP) in NGRIP, 111.44 ± 0.69 ka BP in MON, and 112 $^{+0.52}$ / $_{-0.59}$ ka in BMS1. Within the inherent absolute age uncertainties associated with each chronology, one could assume a quasi-synchronous proxy response to climate change in these three records; however, possible discrepancies in the timing of the climatic response of less than ca. 3000 years (2.5% age uncertainty in NGRIP) cannot be excluded. In order to avoid the effects of the relatively large uncertainties in absolute ages, we apply an alternative approach for the hemispheric-scale comparison. Instead of absolute ages, we compare the duration of the climatic periods in the proxy records from MON, Bue Marino Cave and Greenland, assuming that uncertainties are lower. We consider this as a more suitable approach to identify possible regional differences between Greenland and the Mediterranean. The duration of GI-25b (500 ± 40 years), the cold-dry phase in BMS1 (480 $^{+730}/_{-380}$ years) and MON 1 (440 ± 9 years) are very similar; however, the following warm-wet phase in BMS1 (1080 $^{+850}/_{-630}$ years) and the 'MON rebound-1' (550 ± 35 years) are significantly longer than GI-25a (300 ± 40 years) (Fig. 5; Table 2). A shorter climate rebound in Greenland might suggest that the impact of the cooling at the

362 onset of GS-25 on the Mediterranean region was delayed by at least 250 years given minimum
363 difference between the duration of the rebound phase in Greenland (ca. 300 years) and MON
364 (ca. 550 years calculated in MON). However, we are aware that the sub-events within GI-25
365 in NGRIP are only defined by $\delta^{18}O$ data and the estimated durations were considered as
366 preliminary (Rasmussen et al., 2014). Therefore, the speculation of a possible time lag needs
367 to be tested by other proxy records and improved dating.
368 From 111.4 ka BP (MON 1) back to 120 ka BP, our proxies do not show any significant
369 fluctuations in MON (Fig. 3) that might correlate with GS-26 at 119.14 b2k (Rasmussen et al.,
370 2014). A lower amplitude of this stadial could explain the lack of signal in the MON sediment
371 record as the interglacial environment around the lake was most likely too stable to respond
372 to it. Consequently, the short-lived cooling phase GI-25b recorded in NGRIP at 111.44 ± 2.8 ka
373 b2k was the first of a series of millennial- to centennial-scale high-latitude cold phases that
374 caused environmental responses in the MON record. We suggest this as the beginning of
375 teleconnection between climate variability at northern high latitudes and environmental
376 changes in the Mediterranean that persisted during the entire following glacial period (Allen
377 et al., 1999). This agrees with the evidence for the onset of the global climatic re-organisation
378 at GI-25a (Capron et al., 2012). In contrast to our finding, it has been reported that millennial-
379 scale variability persisted also during the last interglacial in the North Atlantic Ocean
380 (McManus et al., 2002; Wang and Mysak., 2002; Oppo et al., 2006) and in southern Europe
381 (Couchoud et al., 2009; Tzedakis et al., 2018).). It has been therefore proposed that DO-type
382 variability during the last glacial period could have been a continuation of last interglacial
383 millennial-scale variability (e.g. Mokeddem et al., 2014 and Tzedakis et al., 2018). Since these
384 regional comparisons are generally based on proxy wiggle matching possible, regional
385 differences might have been overlooked. Nonetheless, the lack of signal in MON might be
386 explained by the location of Lake Monticchio in a sheltered location within a volcanic crater
387 with favourable local climate conditions. Thus, the amplitude of climatic oscillations during

388 the last interglacial might have been too low to affect the stable forested environment during
389 the last interglacial in southern Italy, or else as during the Holocene (Allen et al, 2002) these
390 oscillations may have acted as triggers for vegetation changes rather than driving fluctuations
391 in the vegetation. It further remains elusive why also the Greenland ice core records do not
392 show such a pronounced millennial-scale variability.
393
394 **5 Conclusions**
395 This study updates the palaeoclimatic and environmental interpretation of the sediment
396 record of Lago Grande di Monticchio, southern Italy, at the transition from the last interglacial
397 to the early glacial.
398 We re-define the short-lived cold phase MON 1 from 111.44 to 111.01 ± 0.69 ka BP. This
399 interval of 440 ± 9 years is characterised by increased varve thickness and formation of siderite
400 varves and includes a brief decline in tree pollen.
401 In contrast to the previous assumptions, we propose that the brief decline in tree pollen at
402 this point in the MON record does not correspond to the Woillard Event. Instead, we consider
403 this abrupt and short fluctuation from 111.177 to 111.150 ± 0.69 ka BP as an episode of low
404 tree pollen production during a more persistently cold episode within the cold phase MON 1.
405 Comparison of the high-resolution sediment proxies and pollen data from the record of Lago
406 Grande di Monticchio has enabled us to identify the onset of environmental response to rapid
407 climatic variability of the last glacial period in the Mediterranean. The first sign of climatic
408 instability in the final phase of the last interglacial appears at 111.44 ± 0.69 ka BP with the
409 onset of MON 1, when siderite varves start forming in response to cooler and drier conditions.
410 MON 1 coincides with the sub-event GI-25b at 111.44 ka b2k with a duration of 500 ± 40 years.
411 Subsequent climate and environmental change in the Mediterranean corresponded to
412 Greenland climate variability on millennial to centennial time scales. Before MON 1, no clear
413 proxy evidence for marked environmental fluctuations is found in the MON sediment record

of the LI. North Atlantic marine records and a Mediterranean speleothem show, however, climatic oscillations also during the last interglacial.

Acknowledgements

This study was funded by the GFZ German Research Centre for Geosciences, Potsdam, Germany, and is a contribution to the Helmholtz Association climate initiative REKLIM (Topic 8 “Rapid Climate Change from Proxy data”). Currently, Celia Martin-Puertas is a Dorothy Hodgkin research fellow funded by the Royal Society (ref: DH150185).

References

Allen, J. R. M., Brandt, U., Brauer, A., Hubberten, H., Huntley, B., Kraml, M., Mackensen, A., Mingram, J., Negendank, È. F. W., Nowaczyk, N. R., Watts, W. A., Wulf, S., and Zolitschka, B. 1999. Rapid environmental changes in southern Europe during the last glacial period. Nature 400, 740–743.

Allen, J. R. M., Watts, W. A., McGee, E., and Huntley, B. 2002. Holocene environmental variability - the record from Lago Grande di Monticchio, Italy. Quat. Int.l 88, 69–80.

Allen, J. R. M. and Huntley, B. 2009. Last Interglacial palaeovegetation, palaeoenvironments and chronology: a new record from Lago Grande di Monticchio, southern Italy. Quaternary Sci. Rev. 28, 1521–1538.

Barker, S., Knorr, G., Edwards, R.L., Parrenin, F., Putnam, A.E., Skinner, L.C., Wolff, E., Ziegler, M. 2011. 800,000 years of abrupt climate variability. Science 334, 347-351.

Blockley, Simon, Bronk Ramsey, C. Lane, C.L., Lotter, A. 2008. Improved age modelling approaches as exemplified by the revised chronology for the Central European varved lake Soppensee. Quat. Sc. Rev. 27, 61-71.

Boch, R., Cheng, H., Spötl, C., Edwards, R. L., Wang, X., and Häuselmann, Ph. 2011. NALPS: a precisely dated European climate record 120–60 ka. Clim. Past 7, 1247–1259.

440 Brauer, A., Allen, J. R. M., Mingram, J., Dulski, P., Wulf, S., and Huntley, B. 2007. Evidence for
441 last interglacial chronology and environmental change from Southern Europe. P. Natl. Acad.
442 Sci. 104, 450–455.
443 Brocchini, D., La Volpe, L., Laurenzi, M. A., and Principe, C. 1994. Storia evolutiva del Monte
444 Vulture. Plinius 12, 22–25.
445 Broecker, W.S. 1998. Paleocean circulation during the last deglaciation: A bipolat seesaw?
446 Paleocenaography 13, 119-121.
447 Bronk Ramsey, C. 2008. Depositional models for chronological records. Quat. Sc. Rev. 27, 42-
448 60.
449 Capron, E., Landais, A., Chappellaz, J., Buiron, D., Fischer, H., Johnsen, S.J., Jouzel, J.,
450 Leuenberger, M., Masson-Delmotte, V., Stocker, T.F. 2012. A global picture of the first
451 abrupt climatic event occurring during the last glacial inception. Geophys. Res. Let. 39,
452 L15703, doi:10.1029/2012GL052656.
453 Chapman, M. R. and Shackleton, N. J. 1999. Global ice-volume fluctuations, North Atlantic ice-
454 rafting events, and deep-ocean circulation changes between 130 and 70 ka. Geology 27,
455 795–798.
456 Cheddadi, R., Mamakowa, K., Guiot, J., de Beaulieu, J.-L., Reille, M., Andrieu, V., Granoszewski,
457 W., Peyron, O. 1998. Was the climate of the Eemian stable? A quantitavite climate
458 reconstruction from seven European pollen records. Palaeogeog. Palaeocl. Palaeoec. 143,
459 73-85.
460 Columbu, A., Drysdale, R., Capron, E., Woodhead, J., De Waele, J., Sanna, L., Hellstrom, J., Bajo,
461 P. 2017. Early last glacial intra-interstadial climate variability recorded in a Sardinian
462 speleothem. Quat. Sc. Rev. 169, 391-397.

463 Couchoud, I., Genty, D., Hoffmann, D., Drysdale, R., Blamart, D. 2009. Millennial-scale climate
464 variability during the Last Interglacial recorded in a speleothem from south-western France.
465 Quat. Sc. Rev 28: 3263-3274.

466 Davis, M.B., Brubaker, L.B., Webb III, T. 1972. Calibration of absolute pollen infux, in: H.J.B.
467 Birks, R.G. West (Eds.), Quaternary Plant Ecology, The 14th Symp. of the British Ecological
468 Society, Blackwell Scienti¢c Publications, University of Cambridge, pp. 9-25.

469 Drysdale, R. N., Zanchetta, G., Hellstrom, J. C., Fallick, A. E., McDonald, J., and Cartwright, I.
470 2007. Stalagmite evidence for the precise timing of North Atlantic cold events during the
471 early last glacial. Geology 35, 77–80.

472 Giaccio, B., Nomade, S.,Wulf, S., Isaia, R., Sottili, G., Cavuoto, G., Galli, P., Messina, P., Sposato,
473 A., Sulpizio, R., and Zanchetta, G.2012. The late MIS 5 Mediterranean tephra markers: a
474 reappraisal from peninsular Italy terrestrial records. Quat. Sci. Rev. 56, 31–45.
475 Hicks, S and Hyvärinen, H. 1999. Pollen infux values measured in different sedimentary
476 environments and their palaeoecological implications. Grana 38, 228-242.
477 Huusko, A. and Hicks, S. 2009. Conifer pollen abundance provides a proxy for summer
478 temperature: evidence from the latitudinal forest limit in Finland. J. Quat. Sci. 24, 522-528.
479 Hutchinson, G.E.ed. 1970. IANULA: an account of the history and development of the Lago
480 Grande di Monterosi, Latium, Italy. Trans. Am. Phil. Soc. 60, 1-178.
481 Kukla, G., McManus, J.F., Rousseau, D-D., Chuine, I. 1997. How long and how stable was the
482 last interglacial? Quat. Sci. Rev. 16, 605–612.
483 Lehman, S.J., Sachs, J.P., Crotwell, A.M., Keigwin, L.D., Boyle, E.A. 2002. Relation of subtropical
484 Atlantic temperature, high-latitude ice rafting, deep water formation, and European
485 climate 130,000-60,000 years ago. Quat. Sci. Rev 21, 1917-1924.

McManus, J. F., Bond, G. C., Broecker, W. S., Johnsen, S., Labeyrie, L., and Higgins, S. 1994. High-resolution climate records from the North Atlantic during the last interglacial, Nature 371, 326–329.

McManus, J.F., Oppo, D.W., Keigwin, L.D., Cullen, J.L., Bond, G.C. 2002. Thermohaline circulation and prolonged interglacial warmth in the North Atlantic. Quat. Res. 58, 17-21.

Martin-Puertas, C., Brauer, A.,Wulf, S., Ott, F., Lauterbach, S., Dulski, P. 2014. Annual proxy data from Lago Grande di Monticchio (southern Italy) between 76 and 112 ka: new chronological constraints and insights on abrupt climatic oscillations. Clim. Past 10, 2099-2114.

Mokeddem, Z., McManus, J.F., Oppo, D.W. 2014. Oceanographic dynamics and the end of the last interglacial in the subpolar North Atlantic. PNAS 111, 11263-11268.

NGRIP project members. 2004. High-resolution record of Northern Hemisphere climate extending into the last interglacial period, Nature 431, 147–151.

Ohlendorf, C., Bigler, C., Goudsmit, G.-H., Lemcke, G., Livingstone, D.M., Lotter, A., Müller, A., Sturm, M. 2000. Causes and effects of long periods of ice cover on a remote high Alpine lake. J. Limnol. 59, 65-80.

Oppo, D.W., McManus, J.F., Cullen, J.L. 2006. Evolution and demise of the Last Interglacial warmth in the subpolar North Atlantic. Quat. Sci. Rev. 25, 3268-3277.

Rasmussen, S.O., Bigler, M., Blockley, S.P., Blunier, T., Buchardt, S.L., Clausen, H.B., Cvijanovic, I., Dahl-Jensen, D., Johnsen, S.J., Fischer, H., Gkinis, V., Guillevic, M., Hoek, W.Z., Lowe, J.J., Pedro, J.B., Popp, T., Seierstad, I.K., Steffensen, J.P., Svensson, A.M., Vallelonga, P., Vinther, B.M., Walker, M.J.C., Wheatley, J.J., Winstrup, M., 2014. A stratigraphic framework for abrupt climatic changes during the Last Glacial period based on three synchronized Greenland ice-core records: refining and extending the INTIMATE event stratigraphy. Quat. Sci. Rev. 106, 14-28.

Regattieri, E., Giaccio, B., Nomade, S., Francke, A., Vogel, H., Drysdale, R.N., Perchiazzi, N.,

512 Wagner, B., Gemelli, M., Mazzini, I., Boschi, C., Galli, P., Peronace, E. 2017. A Last Interglacial
513 record of environmental changes from the Sulmona Basin (central Italy). Palaeogeogr.
514 Palaeocl. Palaeoec. 472, 51-66.

515 Sánchez Goñi, M. F., and Harrison, S. 2010. Millennial-scale climate variability and vegetation
516 changes during the Last Glacial: concepts and terminology. *Quat. Sci. Rev.* 29, 2823–2827.

517 Sánchez Goñi, M. F., Loutre, M. F., Peyron, O., Santos, L., Duprat, J., Malaizé, B., et al. 2005.
518 Increasing vegetation and climate gradient in Western Europe over the Last Glacial
519 Inception (122-110 ka): data-model comparison. *Earth Planet. Sci. Lett.* 231, 111–130.

520 Shackleton, N.J., Chapman, M., Sánchez-Goñi, M.F., Pailler, D., Lancelot, Y. 2002. The Classic
521 Marine Isotope Substage 5e. Quat. Res. 58, 14-16.

522 Shackleton, N. J., Sánchez Goñi, M. F., Pailler, D., and Lancelot, Y. 2003. Marine isotope
523 substage 5e and the eemian interglacial. *Glob. Planet. Change* 757, 151–155.

524 Stoppa, F. and Principe, C. 1998. Erratum to "Eruption style and petrology of a new
525 carbonatitic suite from the Mt. Vulture (Southern Italy): The Monticchio Lakes Formation".
526 J. Volcanol. Geoth. Res. 78, 251–265.
527 Tzedakis, C. 2003. Timing and duration of Last Interglacial conditions in Europe: a chronicle of
528 a changing chronology. Quat. Sci. Rev. 22, 763-768.
529 Tzedakis, C., Drysdale, R.N., Margari, V., Skinner, L.C., Menvidel, L., Rhodes, R.H., Taschetto,
530 A.S., Hodell, D.A., Crowhurst, S.J., Hellstrom, J.C., Fallick, A.E., Grimalt, J.O., McManus, J.F.,
531 Martrat, B., Mokeddem, Z., Parrenin, F., Regattieri, E., Zanchetta, G. 2018. Enhanced
532 climate instability in the North Atlantic and souther Europe during the Last Interglacial. Nat.
533 Comm. 9: 4235.

534 Wang, A. and Mysak, L.A. 2002. Simulation of the last glacial inception and rapid ice sheet
535 growth in the McGill Paleoclimate Model. Geophy. Res. Lett. 29, 2102.
536 Woillard, G. 1979. Abrupt end of the last interglacial s.s. in north-east France. Nature 281,
537 558-562
538 Wolff, E. W., Chappellaz, J., Blunier, T., Rasmussen, S. O., and Svensson, A. 2010. Millennial-
539 scale variability during the last glacial: The ice core record. Quat. Sci. Rev. 29, 2828–2838.
540 Wulf, S., Keller, J., Paterne, M., Mingram, J., Lauterbach, S., Opitz, S., Sottili, G., Giaccio, B.,
541 Albert, P. G., Satow, C., Tomlinson, E. L., and Viccaro, M. 2012. The 100-133 ka record of
542 Italian explosive volcanism and revised tephrochronology of Lago Grande di Monticchio.
543 Quat. Sci. Rev. 58, 104–123.
544
545
546
547
548
549
550
551 **Table 1:** P_Sequence parameters linked to the age model shown in Figure 2. Modelled ages
552 are expressed as maximum (from) and minimum (to), confidence intervals (%) are 68%, and
553 mean ages (μ) and errors (σ) are also shown.
554

Name	Unmodelled (BP)					**Modelled (BP)**				
	from	to	%	μ	σ	**from**	**to**	**%**	**μ**	**σ**
Outlier_Model General						-167	171	68.2	4	564
T (5)	-1.135	1.135	68.2	-2.27E-08	1.29081				-0.002315	1.18295
U (0,4)	3.99E-17	4	68.2	2	1.1431	5.32E-17	2.964	68.2	1.96833	1.14351
P_Sequence										
Boundary						120308	119508	68.2	119903	402
Base varve	120288	119501	68.2		386	120308	119508	68.2	119903	402
						120297	119495	68.2	119903	402
X-6 (^{40}Ar/^{39}Ar)	110419	108583	68.2		900	109906	108502	68.2	109209	**697**
X-5 (^{40}Ar/^{39}Ar)	107327	104675	68.2	106001	1300	107379	105611	68.2	106496	876
Boundary						107379	105611	68.2	106496	876

Table 2: Absolute dating and duration of the climatic oscillations discussed in this study given by the independent chronologies associated with the sediment record of Lago Grande di Monticchio, the Bue Marino Cave speleothem BMS1 and NGRIP ice core ($GICC05_{modelext}$).

Climatic oscillation / event	**Lago Grande di Monticchio Italy, Mediterranean**		**Bue Marino** (Columbu et al., 2017) **Sardinia, Mediterranean**		**NorthGRIP** (Wolff et al., 2010; Rasmussen et al., 2014) **Greenland**	
	Age [ka] and 2σ uncertainty	Duration [years]	Age [ka] and 2σ uncertainty	Duration [years]	Age [b2k] and 2σ uncertainty (2.5%)	Duration [years]
MON 1 / GI-25 b	111,446 ± 697	440 ± 9	$112{,}480\ ^{+520}/_{-590}$	$480\ ^{+730}/_{-380}$	111,440 ± 2,786	500 ± 40
MON rebound 1 / GI-25 a	111,013 ± 697	550 ± 35	$111{,}760\ ^{+430}/_{-450}$	$1080\ ^{+850}/_{-630}$	110,940 ± 2,773	300 ± 40

Figure captions:

Figure 1. (a) Location of Lago Grande di Monticchio and other sites mentioned in the text. (b) bathymetry of the lake and coring sites.

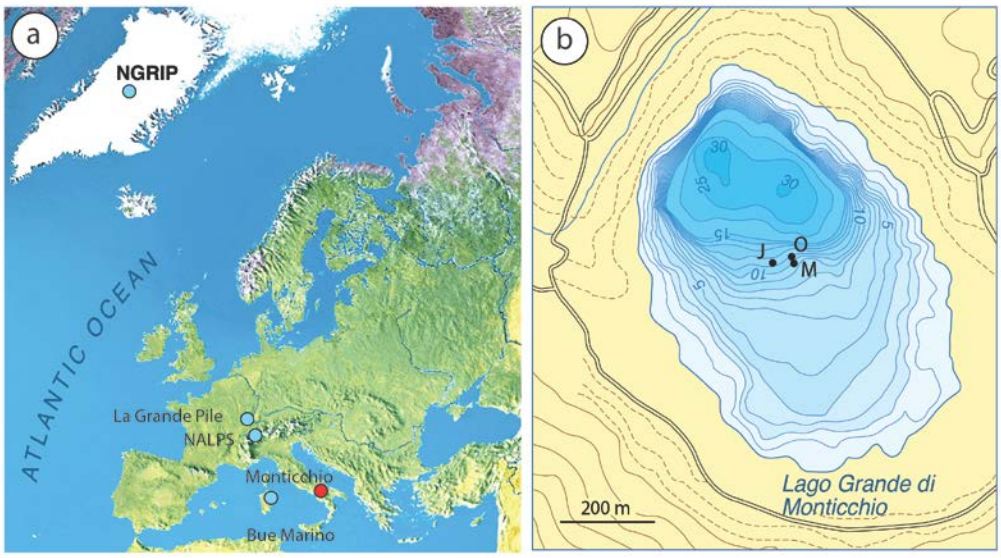

572
573
574
575
576
577
578
579
580
581
582
583
584
585
586

587 **Figure 2.** Age model for Lago Grande di Monticchio during the interval 120–106 ka BP based
588 on varve counts and reported ages for the MON tephras correlated with Mediterranean
589 tephra layers X-5 and X-6. All data were incorporated into a Bayesian P_Sequence age model

with a fixed k value of 0.3 (the model rigidity constraint) and Z defined as relative varve years.

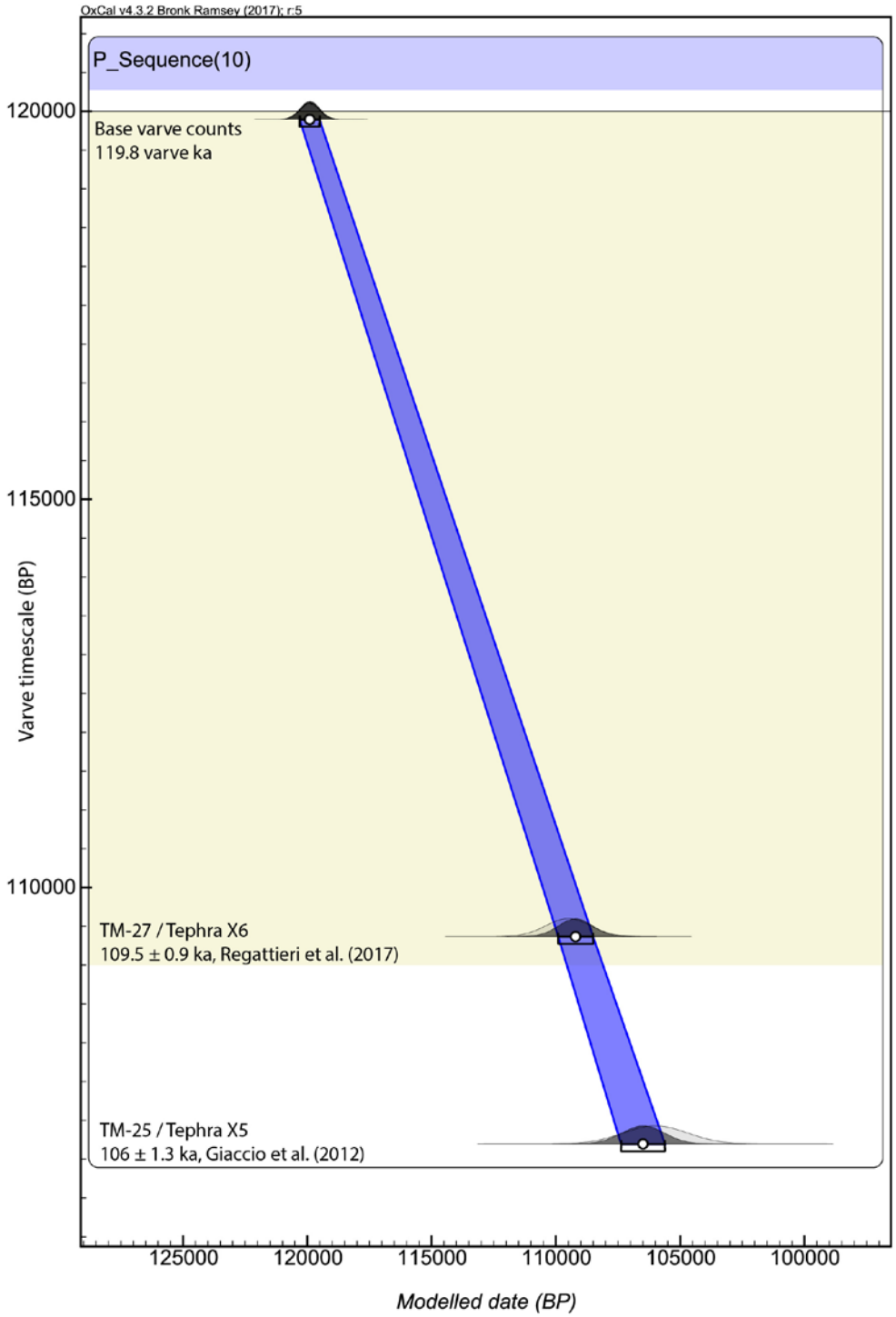

Figure 3. Environmental and climate proxies from the MON sediment record versus age scale. Microscope images of the varved sediments of MON (to left) showing interglacial and glacial varve types; (a) sedimentary units and microfacies; (b) varve thickness; (c) Fe/Ti ratio (log scale); (d) Ti counts; (e) pollen assemblage. Yellow shading indicates the interval MON 1

596 discussed in this study. The dashed line in the middle of the yellow shading shows the position
597 of the pollen anomaly previously identified as the WE. This line also marks the onset of MON
598 1 published by Martin-Puertas et al. (2014), which has been extended in this study.

599

600 **Figure 4.** High-resolution pollen and sediment proxies records during MON 1. (a)
601 Environmental proxies plotted against depth. From left to right: thin section images along the
602 MON 1 oscillation (core M59-u, 17-52 cm); Fe/Ti ratio is plotted on the thin sections images
603 showing an increase in this ratio when siderite varves (light sediments) occur; Woody taxa
604 pollen percentages and woody taxa pollen influx. (b) Environmental proxies plotted against

age. From left to right: varve thickness (log scale); Fe/Ti ratio (log scale); and pollen percentages of woody taxa. Blue points indicate pollen samples published previously in Brauer et al. (2007) and Allen and Huntley (2009), the yellow point corresponds to the WE sample discussed in this study. Red points are the new samples included in this study. Yellow shading indicates the interval MON 1 and grey shading shows the pollen anomaly discussed in the text.

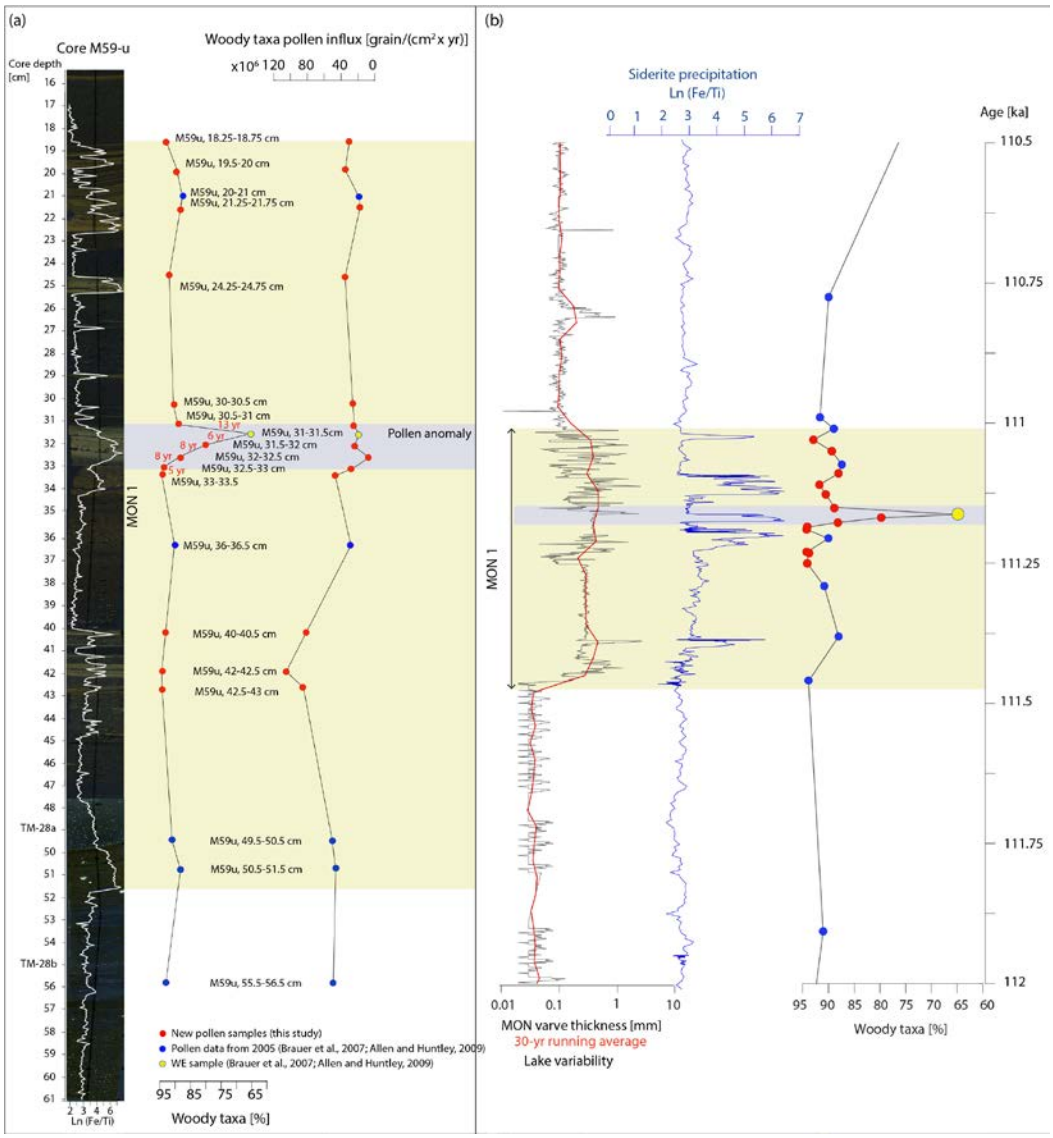

Figure 5. Regional and hemispheric-scale context. Comparison of the MON varve thickness record (centre, c) with the isotope records ($\delta^{18}O$ and $\delta^{13}C$) of the Mediterranean speleothems from Corchia Cave (top, a) and Bue Marino Cave (top, b) and the NGRIP ice core $\delta^{18}O$ record (bottom, d). Each record is plotted using its own chronology. Durations of the relevant intervals are shown.